PHYSICAL REVIEW E **74**, 045602(R) (2006)

Relativistic attosecond electron pulses from a free-space laser-acceleration scheme

Charles Varin* and Michel Piché
Centre d'optique, photonique et laser, Université Laval, Québec, Qc, Canada, G1K 7P4
(Received 16 September 2005; revised manuscript received 1 February 2006; published 20 October 2006)

In this paper we describe how relativistic attosecond electron pulses could be produced in free space by ultrafast and ultraintense transverse magnetic (TM) laser beams. Numerical solutions of the time-dependent three-dimensional Maxwell-Lorentz equations reveal that electrons initially at rest at the waist of a multi-TW pulsed TM_{01} laser beam can be accelerated to multi-MeV energies. The use of a few-cycle laser beam and a compact initial electron cloud forces the particles to effectively interact with a single half-cycle of the laser field and form a pulse of attosecond duration.

DOI: 10.1103/PhysRevE.74.045602 PACS number(s): 41.20.−q, 41.75.Jv, 41.75.Ht

The emerging field of attosecond science offers the possibility of probing molecular dynamics on a timescale comparable to that of electronic processes [1,2]. Nowadays, attosecond pulses are produced via high-harmonic generation using ultrafast (few-cycle) laser pulses; the spectrum of these harmonics extends from the uv to the x rays [3,4]. Such photons are known to have a relatively low probability of interaction with atoms; using recollision electrons, instead of photons, offers practical advantages [5]. In recent years, methods have been developed to generate femtosecond electron pulses of multi-keV energies; these electron pulses have been used to probe the dynamics of phase transitions [6]. In this paper, we describe how a well-collimated attosecond electron pulse is formed during the acceleration of free electrons by the longitudinal field of an ultrafast and ultraintense transverse magnetic laser beam. For multi-TW laser power, it is shown that the peak energy is in the multi-MeV range. Such relativistic ultrashort electron pulses would allow to probe atomic and subatomic processes, with a temporal resolution unmatched by electron accelerators presently in use.

The challenge of producing relativistic ultrashort electron pulses with lasers is as follows. To operate a laser-driven accelerator in a traveling-wave configuration, the displacement of charged particles must be synchronized with the phase of the laser field. Optical beams have, in free space, a superluminal phase velocity that limits the synchronous interaction between light and particles to lengths comparable to the Rayleigh distance. To overcome such a limitation, several techniques have been proposed (a short list is provided in Ref. [7]). One avenue is the inverse Cherenkov scheme where the presence of a background medium allows for synchronous acceleration over long distances [8,9]. However, the presence of a medium limits the application of this scheme to low laser intensities. So far, the schemes exploiting laser-driven plasmas have been the most successful [10–13]. Plasma-based acceleration techniques typically produce femtosecond electron pulses [10]. In this paper we describe how attosecond electron pulses can be produced through the direct (nonponderomotive) interaction of electrons with the field of an ultrafast and ultraintense transverse magnetic laser beam; the acceleration scheme is entirely free space and is not limited by material breakdown [7].

Early works on laser acceleration of particles argued that, according to the Lawson-Woodward theorem, no net energy could be acquired by an electron in an unbounded field. Effectively, in the ponderomotive (linear) regime a nonrelativistic electron (of charge $-e$ and rest mass m_e) is subject to a weak acceleration per field cycle so that the global variation of its velocity is $\Delta v \simeq -\frac{e}{m_e}\int_{-\infty}^{\infty} E dt$ [14]; according to simple physical arguments, the time integral of the accelerating electric field E must be vanishingly small [15]. However, in the relativistic regime this does not apply and a substantial amount of energy can be transferred to free electrons due to nonlinear effects [16–19]. The mechanism is now well understood. It has been shown that, while electrons are accelerated towards the beam periphery by the transverse electric field, the $\mathbf{v}\times\mathbf{B}$ term of the Lorentz force bends the trajectories in the direction of the time-average Poynting vector [20]. For linearly polarized TEM_{00} Gaussian beams, electrons are scattered at large angles and no energetic electrons are produced at beam center; this is a severe limitation for applications where well-collimated electron beams are required. The use of a radially polarized TM_{01} beam instead of the TEM_{00} mode may offer proper transverse confinement, while accelerating particles along the beam axis.

A TM_{01} beam can be generated from two cross-polarized TEM_{01} and TEM_{10} Gauss-Hermite modes of identical waists [21,22]. In the paraxial approximation, this particular type of beam is characterized by a doughnut-shaped intensity profile [7,23,24]. At the center of the beam ($r=0$), the transverse field components are null and the longitudinal electric field component reaches its maximum that is equal to $E_0 2\sqrt{2}\exp(1/2)/(k_0 w_0) \simeq 0.742(\lambda_0/w_0)E_0$, where E_0 is the peak amplitude of the transverse electric field component, w_0 is the beam spot size at the beam waist, $k_0=\omega_0/c=2\pi/\lambda_0$ is the wave number with ω_0 being the angular frequency, λ_0 the central wavelength of the spectrum, and c the speed of light in free space. The beam intensity and power are, respectively, $I_0=E_0^2/(2\eta_0)$ and $P=(\pi/2)\exp(1)I_0 w_0^2$, with $\eta_0=120\pi\ \Omega$; the normalized intensity parameter $a_z^2=(4/\pi^2)\eta_0 I_0 \exp(1)(\lambda_0/w_0)^2(e/m_e c\omega_0)^2$ is consequently defined. In terms of the standard normalized parameter $a_0^2=2\eta_0 I_0(e/m_e c\omega_0)^2$ [18,25] it reads $a_z^2 \simeq 0.551(\lambda_0/w_0)^2 a_0^2$. According to this definition, $a_z^2=1$ corresponds to the following laser power:

*Electronic address: charles.varin.1@ulaval.ca

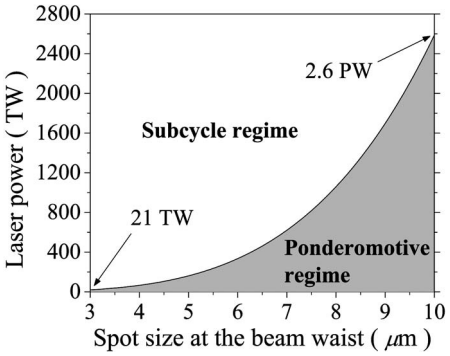

FIG. 1. Power threshold for subcycle electron acceleration to take place along the propagation axis of a TM_{01} beam as a function of the spot size at the beam waist ($\lambda_0=0.8$ μm). The full black line is P^* given at Eq. (1).

$$P^* = (\pi^5/2\eta_0)(w_0/\lambda_0)^4(m_e c^2/e)^2, \tag{1}$$

which marks the transition between the ponderomotive and the subcycle regimes (see Fig. 1).

Electron acceleration by TM_{01} beams in the ponderomotive regime has been extensively studied by Kong *et al.* [26,27], who have shown that trapping and compression of relativistic electron bunches can be achieved. However, due to its time-averaging nature, the ponderomotive interaction between the electrons and the field precludes bunch compression to a timescale much shorter than the laser pulse duration, which is, typically, a few tens of fs. Effectively, attosecond duration is possible if the longitudinal electric component of the TM_{01} beam is strong enough to produce a nonponderomotive acceleration, i.e., if $P > P^*$. The mechanism responsible for electron acceleration in this hyperrelativistic regime has been described in Ref. [7], where we dealt with the one-dimensional equations of motion for a single electron along the propagation axis of a TM_{01} beam. Here, we consider the effective transverse confinement and longitudinal stability (temporal compression) in the subcycle regime using the time-dependent three-dimensional Lorentz equation. For a TM_{01} beam, the Lorentz equation reads

$$d\mathbf{p}/dt = -e[(E_r - v_z B_\theta)\mathbf{a}_r + (E_z + v_r B_\theta)\mathbf{a}_z], \tag{2}$$

where $dp_\theta/dt=0$ due to the particular beam geometry. In the paraxial approximation $B_\theta=E_r/c$. Hence, the transverse force dp_r/dt is proportional to $(1-v_z/c)E_r$: it vanishes at the center of the beam or for relativistic longitudinal velocities ($v_z \simeq c$). However, we recall that for the proposed acceleration scheme electrons are accelerated on axis by the longitudinal component of the electric field E_z (see Ref. [7]): electrons should thus be preferably close to the z axis prior to acceleration. To achieve this task, we propose the use of a nanoparticle placed at the waist of the accelerating TM_{01} beam; this is an alternative to the technique used by Malka *et al.*, where free electrons were created by illuminating a thin film with an intense laser pulse [17]. The illumination of a 10-nm-size nanoparticle by an auxiliary intense laser beam, before the passage of the accelerating TM_{01} beam, could produce a cloud of about 10^5 free electrons, with a dimension growing in time. When driven by ultraintense laser beams, the released electrons behave similarly to electrons initially at rest. To model the acceleration of such an electron cloud, we have considered the trajectories of 2000 electrons whose initial positions in the x-z plane have been chosen randomly using a Gaussian distribution [28] [see Fig. 2(a)]. Electron repulsion was not taken into account due to the small number of particles being considered. We simulated the passage of a 12-fs (FWHM) 100-TW TM_{01} beam. It has thus been observed that, when the diameter of the initial electron cloud is smaller than the wavelength, the particles are captured by the laser field and bunched into a single pulse (see Fig. 2).

It should be noticed that the on-axis phase velocity of the TM_{01} beam is superluminal. However, for $z > z_R$ the dephasing time (the time it takes for a relativistic electron to slip from a field half-cycle to another) is of the order of a few picoseconds (for $w_0=3$ μm at $\lambda_0=0.8$ μm) and grows as

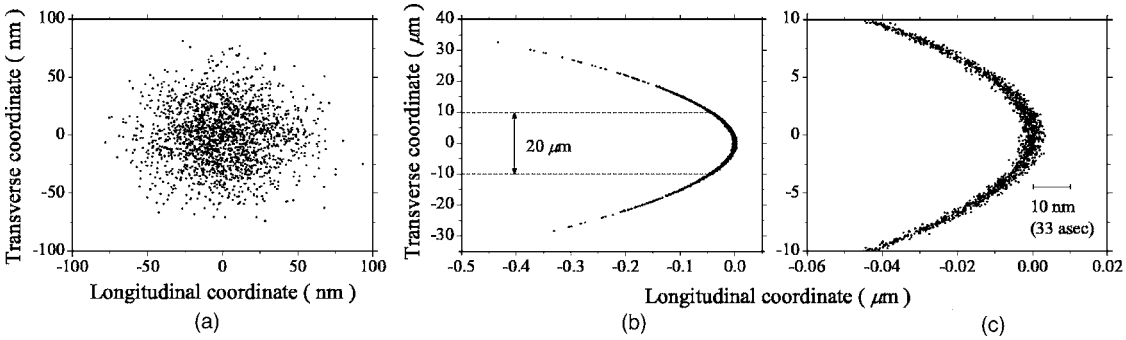

FIG. 2. (a) Spatial distribution of a 100-nm-diameter cloud of 2000 electrons initially at rest at the waist of an ultraintense 12-fs (FWHM) TM_{01} beam. In (b), the same electrons 15 ps after they have interacted with the TM_{01} beam. In (c), a closeup of the front of the electron bunch which reveals its extremely short (attosecond) duration. Parameters used for numerical simulations were $P=100$ TW ($I_0=2.6\times10^{20}$ W/cm^2), $\lambda_0=0.8$ μm, $w_0=3$ μm, and $\phi_0=0.75\pi$ (ϕ_0 is the carrier phase at the waist). The longitudinal coordinate is relative to the position of an electron initially at rest at $z=0$ and accelerated on axis. The origin (0,0) of (b) and (c) thus corresponds to a point located along the z axis at 4.5 mm after the beam waist.

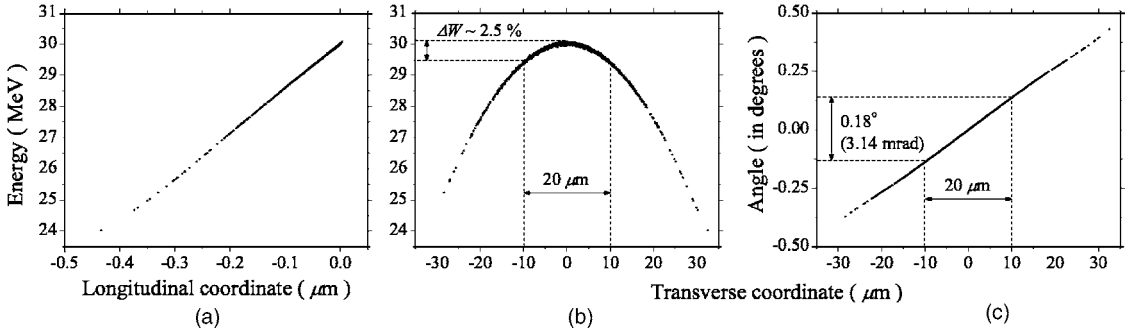

FIG. 3. Energy distribution and divergence of the electrons accelerated by an ultrafast and ultraintense TM_{01} beam at $t=15$ ps. The energy (in MeV) is given as a function of (a) the longitudinal coordinate (see caption of Fig. 2) and (b) the transverse position at the output. In (c) is the angle between the trajectory of each electron and the z axis, given by $\arctan(p_r/p_z)$ evaluated at $t=15$ ps, as a function of the transverse coordinate. Parameters used for the numerical simulations were the same as in Fig. 2.

$\lambda_0(z/w_0)^2/c$ away from the waist ($z_R=k_0w_0^2/2$ is the Rayleigh distance of the beam). Consequently, it appears that, from z_R to ∞, the electrons are kept inside the same accelerating half-cycle; while they are locked to the field phase, they are collectively accelerated. This leads to the parabolic shape—that follows the curvature of the optical wavefront—and attosecond duration of the electron beam (see Fig. 2). In Fig. 3, it is shown that the leading electrons are also the most energetic, with an energy around 30 MeV. These electrons form a dense on-axis pulse with an approximate 20-μm transverse width (FWHM) and a duration (FWHM) below 30 as. We evaluated that the energy spread and the divergence of the electron beam are 2.5% (FWHM) and 1.57 mrad (FWHM), respectively. It should be emphasized that the electron beam divergence is always smaller than that of the laser beam since the electrons are bunched at beam center and are locked to the phase front. For the case we dealt with, we have estimated that the effects caused by electrostatic repulsion are negligible.

We recall that the proposed acceleration scheme is entirely free space. Consequently, it has no limitation regarding to material breakdown at high intensity. According to the acceleration mechanism we described in Ref. [7], the maximum energy that can be acquired by an electron along the axis of an ultrafast and ultraintense TM_{01} beam is given by

$$\Delta W_{\max}[\mathrm{MeV}] = (2\eta_0/\pi)^{1/2}(P[\mathrm{TW}])^{1/2}, \tag{3}$$

where P[TW] is the beam power in TW (10^{12} W) (this calculation includes the effect of the Gouy phase shift). For the results presented in Figs. 2 and 3, the beam power was 100 TW so that $\Delta W_{\max} \simeq 155$ MeV. The electron energy of 30 MeV predicted by the numerical simulations thus represents only 20% of that maximum; when the optimal carrier phase is selected (see Fig. 4) and the position of the initial cloud with respect to the beam waist is optimized (see Fig. 5), the extraction efficiency can be increased to 40%. We observed that, for a single-cycle laser pulse, the final energy approaches $\Delta W_{\max}$. This is explained by the fact that for shorter durations, electrons can reach more easily the center of the laser pulse, where the amplitude of the field is higher. By pulse shaping—for example, by using a pulse with a sharp-rising front—it might be possible to reach the maximum energy with practical pulse durations.

In light of the results presented here, it appears that the experimental demonstration of the proposed direct-field electron acceleration scheme is possible with multi-TW laser beams. The limits of the proposed scheme in terms of the

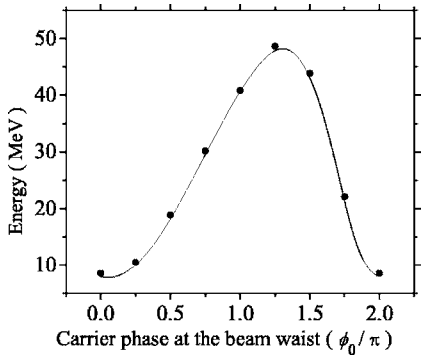

FIG. 4. Energy of the accelerated electrons as a function of the carrier phase at the beam waist. Dots are results obtained from 3D dynamics while the solid curve correspond to an electron initially at rest at $(r,z)=(0,0)$. Parameters used for numerical simulations were the same as in Fig. 2.

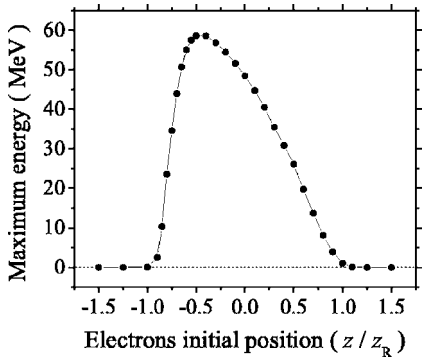

FIG. 5. Energy of the accelerated electrons as a function of their position with respect to the beam waist ($z=0$). Parameters used for numerical simulations were the same as in Fig. 2; ϕ_0 was optimized for maximum energy (see Fig. 4).

duration, divergence, and current of the electron beam are presently under investigation. Preliminary results indicate that it might be possible to produce sub-as electron pulses, though these pulses would be subject to significant space-charge forces that could lead to temporal spreading. According to scaling laws, GeV electrons could be obtained at multi-PW power [7]. We are currently considering different methods to implement acceleration staging in the subcycle regime to reach GeV energies with multi-TW laser power.

This work was supported by Les fonds de recherche sur la nature et les technologies (Québec), the Natural Sciences and Engineering Research Council (Canada), and the Canadian Institute for Photonic Innovations.

[1] M. Hentschel *et al.*, Nature (London) **414**, 509 (2001).
[2] J. Itatani *et al.*, Nature (London) **432**, 867 (2004).
[3] P. B. Corkum, Phys. Rev. Lett. **71**, 1994 (1993).
[4] G. A. Reider, J. Phys. D **37**, R37 (2004).
[5] H. Niikura *et al.*, Nature (London) **417**, 917 (2002).
[6] B. J. Siwick *et al.*, Science **302**, 1382 (2003).
[7] C. Varin, M. Piché, and M. A. Porras, Phys. Rev. E **71**, 026603 (2005).
[8] M. A. Piestrup *et al.*, J. Appl. Phys. **46**, 132 (1975).
[9] J. A. Edighoffer, W. D. Kimura, R. H. Pantell, M. A. Piestrup, and D. Y. Wang, Phys. Rev. A **23**, 1848 (1981).
[10] T. Katsouleas, Nature (London) **431**, 515 (2004).
[11] S. P. D. Mangles *et al.*, Nature (London) **431**, 535 (2004).
[12] C. G. R. Geddes *et al.*, Nature (London) **431**, 538 (2004).
[13] J. Faure *et al.*, Nature (London) **431**, 541 (2004).
[14] E. J. Bochove, G. T. Moore, and M. O. Scully, Phys. Rev. A **46**, 6640 (1992).
[15] K. J. Kim, K. T. McDonald, G. V. Stupakov, and M. S. Zolotorev, Phys. Rev. Lett. **84**, 3210 (2000).
[16] F. V. Hartemann *et al.*, Phys. Rev. E **51**, 4833 (1995).
[17] G. Malka, E. Lefebvre, and J.-L. Miquel, Phys. Rev. Lett. **78**, 3314 (1997).
[18] B. Quesnel and P. Mora, Phys. Rev. E **58**, 3719 (1998).
[19] J. X. Wang *et al.*, Phys. Rev. E **58**, 6575 (1998).
[20] H. Hora *et al.*, Laser Part. Beams **18**, 135–144 (2000).
[21] S. C. Tidwell, D. H. Ford, and W. D. Kimura, Appl. Opt. **29**, 2234 (1990).
[22] R. Dorn, S. Quabis, and G. Leuchs, Phys. Rev. Lett. **91**, 233901 (2003).
[23] A. Siegman, *Lasers* (University Science, Mill Valley, CA, 1986).
[24] C. Varin, M. Piché, and M. A. Porras, J. Opt. Soc. Am. A **23**, 2027 (2006).
[25] T. W. B. Kibble, Phys. Rev. **150**, 1060 (1966).
[26] Q. Kong *et al.*, Phys. Plasmas **10**, 4605 (2003).
[27] Q. Kong *et al.*, Phys. Rev. E **69**, 056502 (2004).
[28] W. H. Press *et al.*, *Numerical recipes in C, The Art of Scientific Computing*, 2nd ed. (Cambridge University Press, Cambridge, 1992).